Filtering Whitewater with an Ultrafiltration Membrane: Effects of the Interaction between Dissolved Organics and Metal Ions on Membrane Fouling

Wenpeng Su, Chen Chen, Hui Xu, Weisheng Yang, and Hongqi Dai*

The mechanisms regarding the influence of dissolved organics in papermaking whitewater together with metal ions on the fouling of an ultrafiltration (UF) membrane were studied in this paper. A series of experiments were carried out to characterize the organic matters' size and membrane flux. The associated fouling mechanism was investigated using the modified Hermia empirical model, resistance distribution, and specific resistance of the cake layer. The results indicated that the addition of metal ions aggravated membrane fouling. Increasing concentrations of metal ions resulted in the higher specific resistance of the cake layer and greater membrane fouling due to their chelation with dissolved organics. Increased pH values influenced the interaction between the metal ions and dissolved organics, resulting in a relatively slow membrane flux decline. Increasing concentrations of Na^+ resulted in greater membrane fouling. Cake layer formation played a major role in treating the water samples with high-concentration metal ions, whereas intermediate blocking formation may be the dominant fouling mechanism when treating the solution without metal ions.

Keywords: Whitewater; Metal ions; Dissolved organics; Membrane fouling mechanism

*Contact information: Jiangsu Provincial Key Lab of Pulp and Paper Science and Technology, Nanjing Forestry University, Nanjing 210037, China; *Corresponding author: hgdhq@njfu.edu.cn*

INTRODUCTION

Increased closure of whitewater systems in the papermaking industry is being carried out progressively to reduce effluent discharge and fresh water consumption (Wu *et al.* 2014). In other words, process water in a typical paper machine system is being recycled multiple times for various purposes. However, the accumulation of dissolved and colloidal substances (DCS) in this process tends to interfere with the papermaking process (Tenno and Paulapuro 1999; Ashrafi *et al.* 2015). Meanwhile, the interaction between DCS and added cationic chemicals affects the product quality (Pokhrel and Viraraghavan 2004). Previous studies have shown that dissolved organic matter (DOM) is the main component in white water, and includes carbohydrates, lipophilic extractives, and other chemicals that contribute to their higher solubility and stability (Antony *et al.* 2012; Su *et al.* 2015). The removal of DOM from the solution becomes a key problem during the closure of whitewater circuits in the papermaking industry.

Membrane filtration has been extensively studied for industrial effluent treatment. After years of development, membrane technology has developed into a promising technology for the removal of DOM in whitewater. Membrane filtering systems have several advantages over traditional disposal methods, including space and energy savings, better safety, and convenient operation (Kumar *et al.* 2015; Shamsuddin *et al.* 2015).

Nevertheless, membrane fouling is a major obstacle to the successful operation of membrane separation. The permeate flux is hindered because of membrane fouling, resulting in low processing efficiency, high operating costs, and increased cleaning frequency (Guo *et al.* 2012; Jiang *et al.* 2012; Karabelas and Sioutopoulos 2015). So far, many studies on membrane fouling have focused on operational conditions (Wang *et al.* 2008), the characteristics of the membrane (Zhao *et al.* 2015), and solution properties such as the particle size of organic matters and the ionic strength of the feed water (Chen *et al.* 2006; Park *et al.* 2006). A series of studies showed that the surrounding environment, especially metal ions, may be one of the main factors affecting membrane fouling. The solubility and form of the organic molecules can be influenced by metal ions (Kloster *et al*. 2013). Roger reports that the charge and aggregation of organic matter in solutions may be influenced by the monovalent ion and divalent ions (Roger *et al.* 2013). Yoon *et al.* (1998) suggests that inorganic ions can form chelates with organic matters, resulting in the adsorption of organics on the membrane surface. Some studies found that the pH values and metal ions could affect the characteristics of organic substances, retention in the membrane, and membrane permeability (Chon *et al.* 2013; Feng *et al.* 2013). However, the mechanism by which different organic matters combined with salt ions affect membrane fouling is still unclear. There is a paucity of available information on the influence of interactions between organic matters and metal ions on membrane fouling under different conditions. Therefore, the characteristics of membrane fouling under typical conditions remain a challenge to membrane technology.

To explore the nature of membrane fouling during the ultrafiltration of wastewater, the mechanism of fouling was considered in the light of Hermia's model. Moreover, the specific resistance of a cake layer was suggested to measure the degree of cake formation on the membrane surface, evaluating the impact of different metal ions' concentration on membrane fouling (Tang *et al.* 2014). In this work, the aim was to study the effects of various ions (Na^+, Ca^{2+}, and Fe^{3+}) on the membrane fouling behavior of DOM in whitewater. The fouling mechanisms were analyzed using Hermia's model, the resistance distribution of the membrane, and the specific resistance of the cake layer. This study lays a primary investigation for the formation of membrane fouling filtering whitewater with various metal ions, and gives theoretical support to interactions between various metal ions and DOM in papermaking whitewater.

EXPERIMENTAL

Materials

Commercial polyethersulfone (PES) membranes were purchased from Mosu Scientific Equipment Company, Shanghai, China. The PES membrane has a molecular weight cut-off (MWCO) of 10 kDa and an effective surface area of $3.32\times10^{-3}m^2$. The water used was high-quality deionized water (> 15 MΩ cm^{-1}).

Model Foulants

Low molecular weight (MW) sodium polyacrylate (PAAS) accounts for a great proportion of solubilized polymer content in papermaking whitewater according to a previous study (Chai *et al.* 2006; Su *et al*. 2015). Thus, in the present work PAAS (MW 3000 Da) was chosen as a model fouling agent. The stock solution of PAAS (0.25 g/L) was prepared by dissolving the liquid form of PAAS into deionized water. The chemical

environment (pH values, ionic strength, high valence metal ion concentration) of feed waters were adjusted with NaOH (0.1 M), HCl (0.1 M), NaCl (10 mM), $CaCl_2$ (3 mM), and $FeCl_3$ (3 mM). The temperature of samples during the fouling indices experiments was maintained at 25 °C.

Membrane Filtration of DOM Solutions and Characterization

pH values, concentration of metal ions

Analytical grade $CaCl_2$ and $FeCl_3$ were used as the metal ion sources. The concentrations of metal ions in PAAS solutions were 5, 10, 15, 20, and 40 mM, respectively. $CaCl_2$ or $FeCl_3$ was first dissolved in deionized water to obtain a given concentration of metal ions. Then, a small volume of these samples was added to the PAAS solutions to obtain the desired concentrations of metal ions. The water sample with a Ca^{2+} or Fe^{3+} concentration of 5 mM and an Na^+ concentration of 0.1 M was used to study the role of pH on membrane fouling. The pH value was adjusted to 6, 7, and 9 by the addition of 0.1 M HCl. Meanwhile, the water sample with a calcium ion or ferric ion concentration of 5 mM and a pH value of 7 was used to investigate the role of Na^+ concentration on membrane fouling. The Na^+ concentration was adjusted to 0.01 M, 0.05 M, and 0.1 M by the addition 0.1 M NaCl. All these water samples were stirred for 2 h at 25 °C to obtain a homogeneous solution. A laser particle size analyzer was used to determine the size of PAAS.

Membrane fouling experiments

A 300-mL stirred dead-end ultrafiltration (UF) module was used to evaluate the membranes' fouling properties (Fig. 1). The experimental apparatus was equipped with a stirrer that operated at a constant rate (250 rpm). The operating pressure was supplied by pure nitrogen at a constant 0.1 MPa. The filtrate was collected in a glass container. The accumulative permeate volume was automatically recorded by a data acquisition system. The membrane flux was calculated from this data.

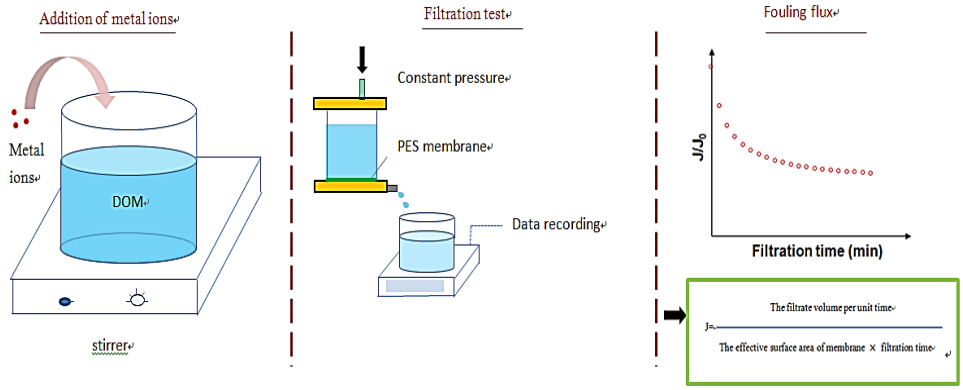

Fig. 1. Schematic of an experimental procedure

In addition, the relative flux (J/J_0) was used to reduce experimental error, where J (L/m^2·h) was the permeate flux and J_0 (L/m^2·h) was the pure water flux. The PAAS rejection, R, was defined as follows,

$$R = \frac{1-C_p}{C_0-C_p} \times 100[\%] \quad (1)$$

where C_p is the PAAS concentration in the permeate, C_0 is the PAAS concentration in the initial feed solution. The concentration of PAAS was determined using a Shimadzu TOC-5000A.

The fouling mechanism can be assessed by Hermia's semi-empirical model under the condition of dead-end filtration. Four basic fouling types of this model were expressed by Eqs. 2 through 5, respectively (Baguena *et al.* 2015):

Complete blocking model: $$\mathrm{Ln}J = \mathrm{Ln}J_0 - k_1 t \quad (2)$$

Standard blocking model: $$1/J^{0.5} = 1/J_0^{0.5} + k_2 t \quad (3)$$

Intermediate blocking model: $$1/J = 1/J_0 + k_3 t \quad (4)$$

and

the cake layer blocking model: $$1/J^2 = 1/J_0^2 + k_4 t \quad (5)$$

where J (L/m^2·h) is the permeate flux, J_0 (L/m^2·h) is the pure water flux, t is the filtration time (min), and k_1, k_2, k_3, and k_4 are constants of the model. The main fouling mechanism can be confirmed according to the relevant correlation coefficients (R^2) by calculating the experimental data into these formulas. A larger R^2 value indicates a better fitting model.

Fouling resistance determination

The membrane fouling was influenced by several factors, including the formation of a cake layer, the concentration polarization on the membrane surface, and pore blocking. The distribution of different filtration resistances can be used to analyze the types of membrane fouling. In this study, the filtration resistances R_m (the intrinsic membrane resistance), R_a (the adsorption resistance), R_g (the pore blocking resistance), R_c (the cake resistance), and R_{cp} (the concentration polarization resistance) were measured. The filtration resistances were calculated using Eqs. 6 through 10 (Listiarini *et al.* 2009; Rajabi *et al.* 2015):

$$R_m = \Delta P/\mu J_i \quad (6)$$

$$R_a = \Delta P/\mu J_a - R_m \quad (7)$$

$$R_g = \Delta P/\mu J_f - R_m - R_a \quad (8)$$

$$R_c = \Delta P/\mu J_v - R_m - R_a - R_g \quad (9)$$

and

$$R_{cp} = \Delta P/\mu J_l - R_m - R_c - R_g - R_a \quad (10)$$

where J_i is the pure water flux through a new membrane (L/m^2·h); J_a is the pure water flux through the membrane after the static adsorption of organics from the processing water (L/m^2·h); J_f is the pure water flux through the membrane, where surface contamination of the membrane adsorbed from the process water was eliminated beforehand (L/m^2·h); J_v is the flux achieved at the end of ultrafiltration (L/m^2·h); J_l is the raw water flux through the membrane after the static adsorption of organics from the process water (L/m^2·h); ΔP is the applied trans-membrane pressure (Pa); and μ is the viscosity of fresh water (Pa·s).

Scanning electron microscopy (SEM) and SEM-EDS analysis of membranes

The detailed structural information regarding the membranes was examined with scanning electron microscopy, using a filament voltage of 20 keV. Dry membrane samples were dispersed on a graphite ribbon fixed on an aluminum sample holder. The powders were sputter-coated with gold in a modular high-vacuum coating system Q150R ES (Quorum Technologies, Japan). The EDS was used to determine the elemental composition of foulants present on the membrane's surface.

The surface charge of PES membranes

To evaluate the surface charge of the PES membrane at different pH values, the surface zeta potentials of the membranes were measured with a SurPASS electrokinetic analyzer (Antor-Paar Gmbh) in the pH range 5 to 9. The surface zeta potential (δ) of the membranes was calculated using the Helmholtz-Smoluchowski equation,

$$\delta = \frac{\Delta E_{sp}}{\Delta P'} \times \frac{\eta \kappa}{\varepsilon_0 \varepsilon_r} \quad (11)$$

where $\Delta E_{sp}/\Delta P'$ is the change in streaming potential with pressure, η is the viscosity of the electrolyte, κ is the conductivity of the electrolyte, and ε_r and ε_0 are the permittivity of the electrolyte and free space, respectively.

RESULTS AND DISCUSSION

Influence of Metal Ions on Membrane Fouling at Different pH Values

The particle size of PAAS is an important parameter in membrane fouling since it can affect the membrane fouling type, and thereby influence membrane filtration. Figure 2 shows the particle size of PAAS with metal ions (Ca^{2+} or Fe^{3+}) at different pH values.

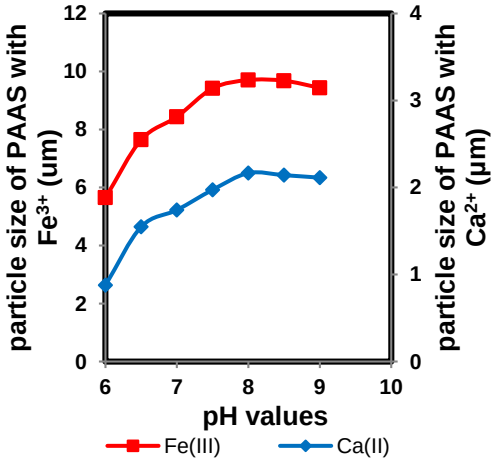

Fig. 2. Effect of pH value on the particle size of organic matter

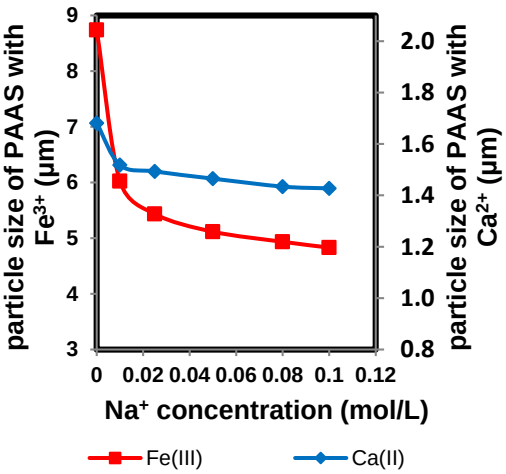

Fig. 3. Effect of Na^+ concentration on the particle size of organic matter

Because of the effects of pH values on the aggregation between PAAS and metal ions, the PAAS size was larger at high pH values than that in the acidic environment. At low pH values, high concentrations of H^+ in the solution competed with metal ions for the active sites of PAAS, reducing the complexation between PAAS and metal ions. Therefore,

the PAAS size at acidic pH values was small. In contrast, PAAS may offer more binding sites to metal ions to bridge adjacent PAAS molecules in an alkaline solution (Garcia *et al.* 2014). The complexation between PAAS and metal ions neutralize the negative charge of PAAS, which results in high levels of aggregation, increasing the particle size of PAAS. In addition, differences between the particle size of PAAS-Ca and PAAS-Fe at the same pH values may relate to the complex strength between PAAS and metal ions. This complexation was affected by several factors such as ionic radii, hydrolysis constant, electronegativity, and electron-shell structure of the metal. What's more, the complexation process may be affected by the density of the ion charge and by the orbital energy valence. (Heidari *et al.* 2013).

The membrane surface properties at different pH values were investigated by zeta potential measurements as presented in Fig. 4. The PES membrane mainly exhibited negative surface charged property over pH ranges from 5 to 9. The PES membrane showed a reduced surface zeta potential within a range from -12.55 mV at pH 5 to -39.28 mV at pH 9.

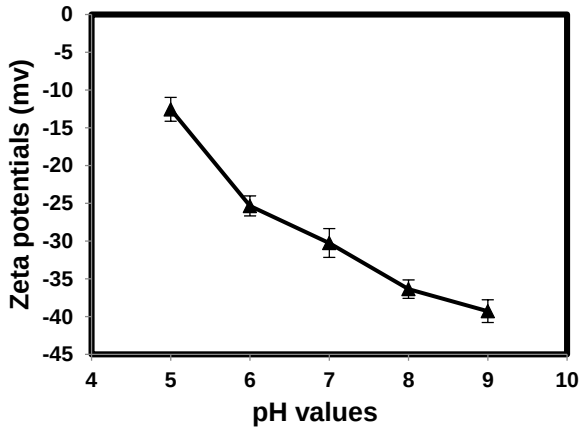

Fig. 4. Surface zeta potential for PES membrane with 200mg/L PAAS loading over pH range of 5-9 using 1mM KCl aqueous solution as electrolyte

A more negatively charged membrane surface could be obtained at higher pH values. Previous studies suggested that high concentrations of H^+ in the solution at acidic pH values could increase the hydrophobicity of the membrane for the neutralization of negative charges on the membrane surface, aggravating membrane fouling (Chen *et al.* 2015; Lin *et al.* 2015). Low pH values tend to cause severe membrane fouling (Fig.5 (a)).

High concentrations of H^+ in the solution may weaken the electrostatic repulsion between the membrane surface and PAAS (Ang *et al.* 2006). At low pH values, mass PAAS particles attached to the membrane surface for weak electrostatic repulsion, reducing the membrane flux.

The amount of PAAS particles adsorbed on the membrane surface decreased at high pH values, tending to mitigate membrane fouling. However, more binding sites were offered at high pH values for the complexation between PAAS and metal ions, increasing the metal ions bridging between PAAS in the solution and in the deposited layer, tending to aggravate membrane fouling (Nguyen *et al.* 2013). As an integrated effect, membrane fouling tended to be aggravated at low pH values.

The filtration resistance distributions of membranes at different pH values are summarized in Table 1. The results indicate that weak electrostatic repulsion between PAAS and the membrane surface at low pH values resulted in higher R_a (adsorption resistance) and R_c (cake resistance). The PAAS particles may be quickly adsorbed on the membrane surface during the initial period of filtration. The cake layer formed at low pH values was more compact than that formed at higher pH values, aggravating membrane fouling.

Table 1. Membrane Resistance Distribution with Simulated Solutions at Different pH Values

Concentration of Ca^{2+}	pH	R_m (m^{-1})	R_a (m^{-1})	R_c (m^{-1})	R_g (m^{-1})	R_{cp} (m^{-1})
5 mM	6	1.73E+13	4.75E+12	3.19E+12	1.33E+11	7.44E+11
	7	1.73E+13	4.04E+12	1.93E+12	6.21E+11	6.18E+11
	9	1.73E+13	3.32E+12	1.26E+12	3.03E+11	1.04E+12

Influence of Metal Ions on Membrane Fouling at Different Na^+ Concentrations

Figure 5 reports the results of the test related to sodium ion concentrations and also at different pH values. As shown in Fig. 5, higher rates of flux decrease were observed at lower pH and with higher NaCl concentration values. As can be seen from Fig. 5(b), PAAS solutions with low Na^+ concentrations did not exhibit an obvious decline in relative flux during filtration. As the Na^+ concentration increased, the decline of filtration flux became more marked. The relative flux at 30 min when filtering PAAS solutions with 0.1 M Na^+ was 0.19, whereas the values for PAAS solution with 0.01 M Na^+ was 0.68. In general, PAAS tended to be less charged at increased salt concentrations, which can be explained by the double layer compression effect. This phenomenon is similar to that reported by Wang *et al.* (2013) Thus, the repulsive forces between the PAAS and the membrane surface decreased at high Na^+ concentrations. Mass organic matters adsorbed on the membrane surface, aggravating the membrane fouling.

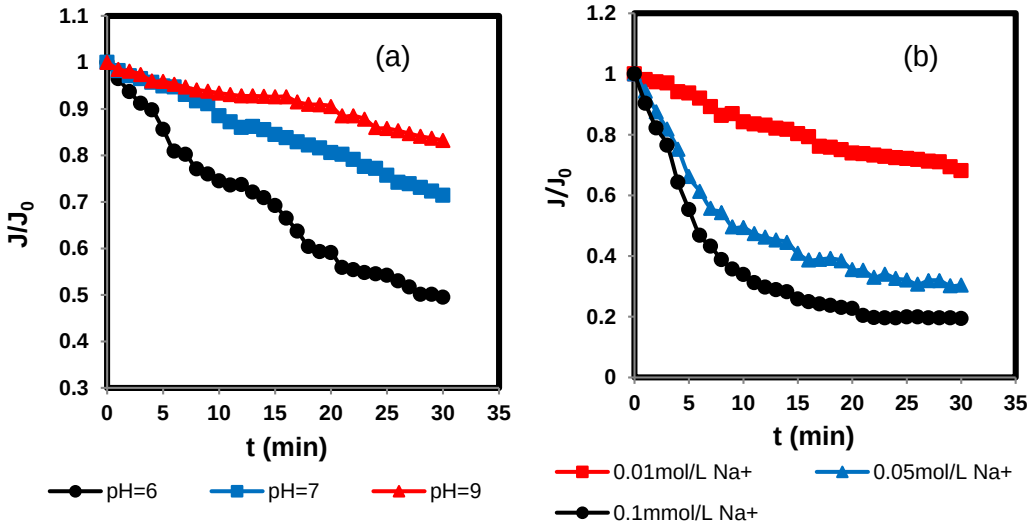

Fig. 5. Effect of pH values and Na+ concentration on membrane flux: (a) effect of pH values on membrane flux; (b) Effect of Na+ concentration on membrane flux. Concentration of PAAS is 200mg/L, other experimental conditions: 10KDa membrane, ΔP=0.1MPa, ionic strength 5mM Fe^{3+}.

Influence of Metal Ion Concentration on Membrane Fouling

Figure 6 shows the particle size of PAAS with metal ions (Ca^{2+} or Fe^{3+}) at different Na^+ concentrations. The Na^+ concentration had an obvious impact on the particle size of PAAS. As can be seen in Fig. 6, the particle size of PAAS decreased with increasing Na^+ concentration. The observed results demonstrate that the particle size of PAAS with 5 mM Fe^{3+} and 0.1 M Na^+ was 4.83 μm, smaller than that of PAAS with 5 mM Fe^{3+} and 0.01 M Na^+ (6.02 μm). This indicates that the concentration of Na^+ had a negative effect on the aggregation of PAAS molecules. High Na^+ concentration in the solution competed with metal ions for the active sites of PAAS, reducing the complexation efficiency between the PAAS and metal ions (Zhang *et al.* 2015).

To study the influence of metal ions on membrane fouling, a series of filtration experiments using model PAAS solutions with various concentrations of metal ions were carried out. The pH values of PAAS solutions were adjusted to 7, and the Na^+ concentration was 0.1 M. The particle size of PAAS in different PAAS-metal ion systems is provided in Fig. 6. The evolution of the ultrafiltration membrane relative flux (J/J_0) is shown in Figs. 7 and 8. As can be seen in Fig. 6, the particle size of PAAS was clearly influenced by the concentration of metal ions (Ca^{2+} and Fe^{3+}). A smaller particle size was seen in the membrane-PAAS system without metal ions. There were repulsive forces between PAAS molecules due to the negative charges of PAAS in water, which resulted in good dispersion of PAAS (Hao *et al.* 2013). The size of organic matter increased with the addition of metal ions. PAAS matter contains carboxylic groups, which bind with metal ions to form large particulates. As shown in Figs. 7 and 8, the addition of metal ions seemed to increase PES membrane fouling.

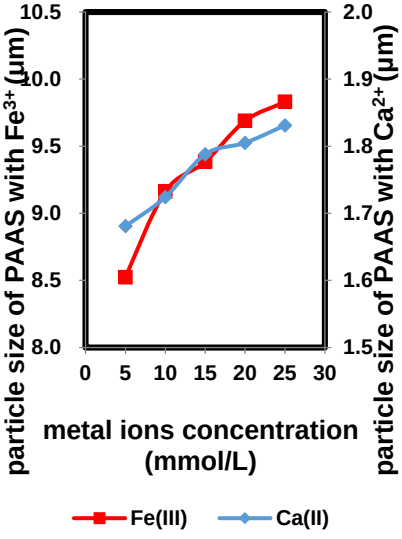

Fig. 6. Effect of Ca^{2+}(Fe^{3+}) concentration on particle size of organic matter

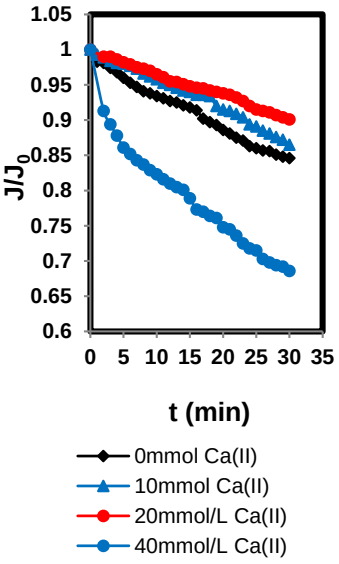

Fig. 7. Effect of Ca^{2+} concentration on membrane flux

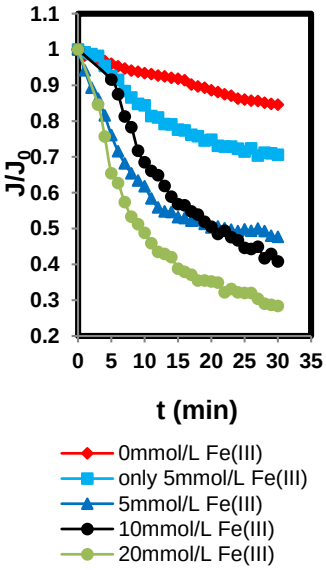

Fig. 8. Effect of Fe^{3+} concentration on membrane flux

The reasons are as follows: firstly, the complexation between PAAS and metal ions became more obvious at high ion concentrations, increasing the metal ions bridging between PAAS in the solution and in the deposited layer. Large organic particles were fixed on the membrane surface. The cake layer that formed in this case was thick and compact, aggravating membrane fouling. Secondly, the addition of metal ions may

neutralize the negative charges on the membrane surface, reducing the electrostatic repulsion between the membrane surface and organic matters, and larger particle foulants may easily attach onto the membrane surface, causing membrane fouling during the early stage of filtration (Habib *et al*. 2013; Zhang *et al*. 2013). The membrane flux decline caused by model PAAS solutions with various concentrations of metal ions was further studied through fouling resistances.

The filtration resistance distributions of membranes at different Na^+ concentrations are summarized in Table 2. The results indicate that weak electrostatic repulsion between PAAS and the membrane surface at high Na^+ concentrations resulted in higher R_a and R_c. Mass PAAS particles adsorbed on the membrane surface during the initial period of filtration. The cake layers that formed at high Na^+ concentrations were more compact, aggravating membrane fouling.

Table 2. Membrane Resistance Distribution with Simulated Solutions at Different Na^+ Concentrations

Concentration of Ca^{2+}	Concentration of Na^+ (M)	R_m (m^{-1})	R_a (m^{-1})	R_c (m^{-1})	R_g (m^{-1})	R_{cp} (m^{-1})
5 mM	0.01	1.73E+13	2.07E+12	1.81E+12	8.15E+11	7.36 E+11
	0.05	1.73E+13	3.45E+12	1.88E+12	6.03E+11	6.00E+11
	0.10	1.73E+13	4.38E+12	2.83E+12	7.62E+11	6.29E+11

As shown in Fig. 9, at different ion concentrations, a close relationship was found between the membrane fouling and the filtration resistances. For the PAAS solution with 40 mM Fe^{3+}, the membrane resistance of R_m comprised a small proportion of the overall resistance (18.17%), but a much higher resistance of cake layer formation was observed (38.94%). High concentrations of metal ions yielded a larger particle size of PAAS and filter cake pollution, which contributes to lower pore-blocking resistance and larger cake resistance. In this case, the membrane flux declined rapidly. In contrast, the model PAAS without metal ions yielded lower cake resistance and less membrane fouling.

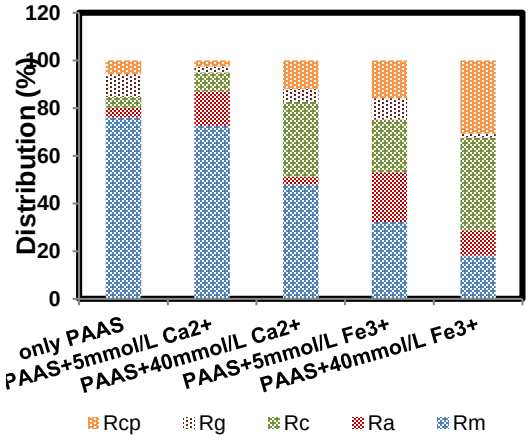

Fig. 9. Membrane resistances when filtering PAAS solutions

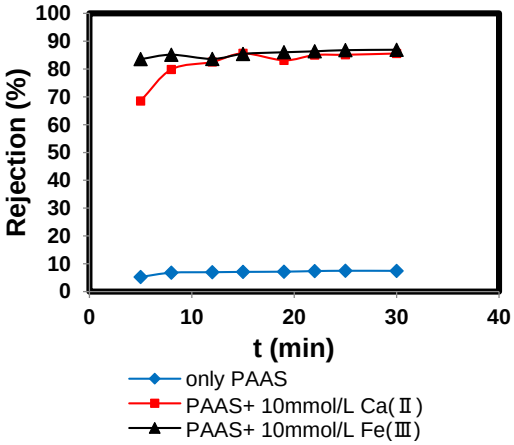

Fig. 10. The rejection of PAAS during ultrafiltration. Concentration of PAAS is 200 mg/L, other experimental conditions: 10 kDa membrane, ΔP= 0.1 MPa

Fouling Mechanism of PAAS on Membrane Fouling at Different Metal Ion Concentrations

The PAAS rejection (*R*) during filtration was studied relative to the fouling mechanism of PAAS at different metal ion concentrations (Fig. 10). The low rejection (~10%) of PAAS showed that the intrinsic pore size of the membrane was large enough to allow most PAAS molecules to pass through. The addition of metal ions (Ca^{2+}, Fe^{3+}) to the feed PAAS solution clearly increased the PAAS rejection. The high rejection of PAAS (~85%) might have been caused by the formation of larger aggregates of PAAS molecules via the creation of Ca^{2+} (Fe^{3+}) bridges the PAAS molecules, and by Ca^{2+} (Fe^{3+}) bridges between the PAAS in solution. Ca^{2+} (Fe^{3+}) might also have formed bridges between the PES membrane and the PAAS molecules.

SEM imaging (Fig. 11(a–d) was used to observe the membrane surfaces fouled with PAAS at different metal ion concentrations. The virgin PES membrane exhibited a smooth surface (Fig. 11(a). After filtration of the PAAS solution without metal ions, a small amount of foulants appeared on the membrane surface (Fig. 11(b)).

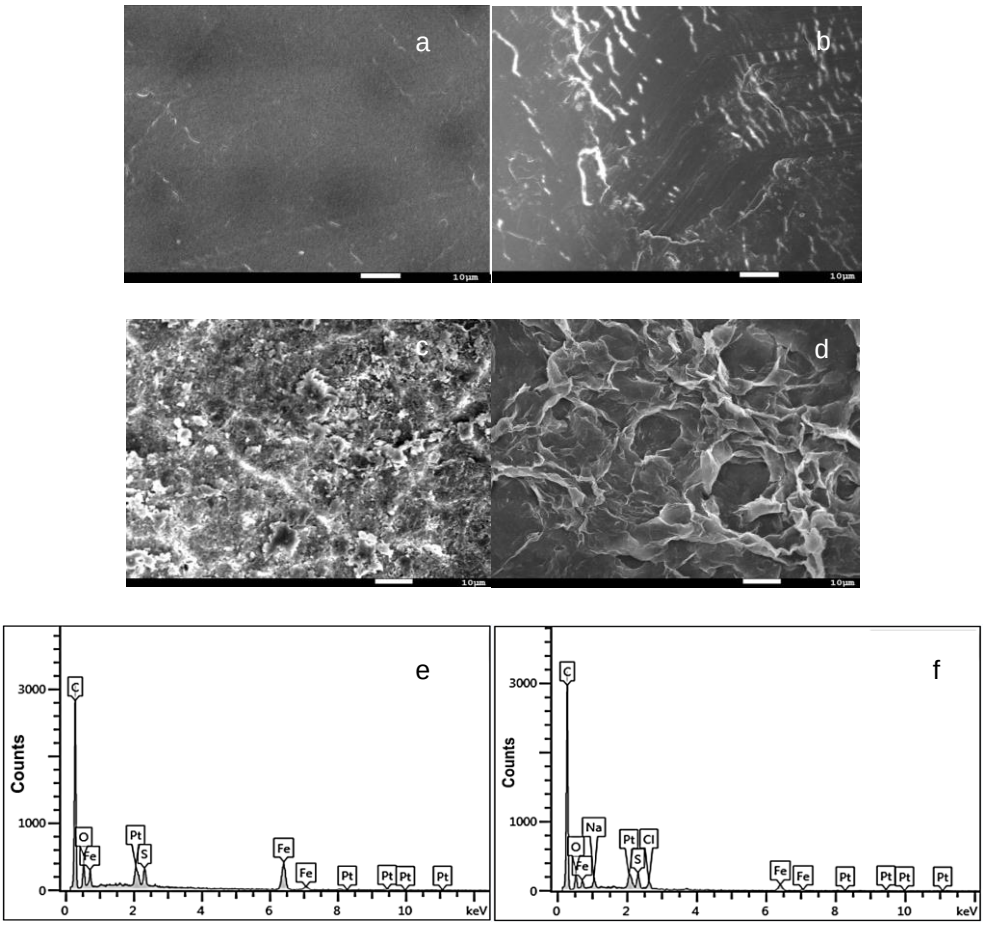

Fig. 11. SEM and EDS analyses of the membrane surface. The surface of the membrane before use (a) Original membrane; (b) Fouled by a 250-mg/L PAAS solution; (c) Fouled by a 250-mg/L PAAS with 5 mM $FeCl_3$; (d) Fouled by a 250-mg/L PAAS with 40 mM $FeCl_3$; (e) EDS spectra of membrane surface fouled by a 5-mM $FeCl_3$ solution; (f) EDS spectra of membrane surface by a 250-mg/L PAAS with 5 mM $FeCl_3$

Interestingly, large amounts of foulants were observed on the membrane surface after the filtration of PAAS with metal ions. For the filtration of PAAS with higher metal ion concentrations, the whole membrane surface was covered by foulants. The cake layer seemed to be more compact and thicker than in other cases. An EDS analysis was performed to determine the elements present on the fouled membrane surfaces. The analysis revealed the presence of Fe on the membrane surface (Fig. 11(e–f)). Compared with the content of Fe on the membrane surface fouled by the 5 mM $FeCl_3$ solutions, the content of Fe was lower on the membrane surface fouled by the PAAS/Fe solutions. This may imply that PAAS molecules surrounded the Fe in the solution, then the PAAS/iron complexes were deposited on the surface of membrane (Hao *et al*. 2013).

To better understand the fouling mechanism of the membrane filtering PAAS solutions with various metal ion concentrations, the membrane flux curves were fitted using Hermia's semi-empirical model. According to the Hermia model, four possible fouling mechanisms need to be considered: complete blocking; intermediate blocking; standard blocking; and gel layer formation (Abdelrasoul *et al.* 2013; Aslam *et al.* 2015). The fouling mechanism can be assessed using Hermia's model under the condition of dead-end filtration (Su *et al.* 2015). The fitted situations (R^2) of the models found by studying the effect of metal ions concentration are shown in Table 3. Intermediate blocking was well-fitted to the experimental results for the PAAS solution without metal ions. In this case, the particle size of PAAS was observed to be low. The membrane pore size was large enough to allow PAAS molecules to enter membrane pores and precipitate onto the pore, causing pore blockage. On the other hand, the highest value of R^2 was obtained for gel layer formation models when the PAAS solution contained a high ion concentration. With increasing concentrations of metal ions, the average particle size of PAAS molecules increased due to the complexation between PAAS and metal ions. Most of the molecules were larger than the membrane pores. The gel-cake formation played a significant role during filtration. Meanwhile, the addition of metal ions may neutralize the negative charge of organic matters, reducing the electrostatic repulsion between PAAS and the membrane surface. Large amounts of complexes were adsorbed on the membrane surface, resulting in severe membrane fouling during the early stage of filtration. Hence, gel layer formation was the dominant mechanism for PAAS solution with high ion concentrations, and intermediate blocking fouling was the major mechanism for the PAAS solution without metal ions.

Table 3. Correlation Coefficient (R^2) for Four Blocking Models Fitting Under Constant Pressure (0.1 MPa)

Metal Ions	Concentration of Metal Ions (mM)	Correlation Coefficient (R^2) of Hermia's Model			
		Complete	Standard	Intermediate	Cake
Ca^{2+}	0	0.9326	0.9330	0.9932	0.9428
	10	0.9882	0.9864	0.9844	0.9899
	20	0.9831	0.9827	0.9822	0.9909
	40	0.9651	0.9731	0.9792	0.9865
Fe^{3+}	0	0.9326	0.9330	0.9932	0.9428
	5	0.8277	0.8541	0.8778	0.9162
	10	0.9660	0.9802	0.9879	0.9837
	20	0.9114	0.9499	0.9760	0.9915

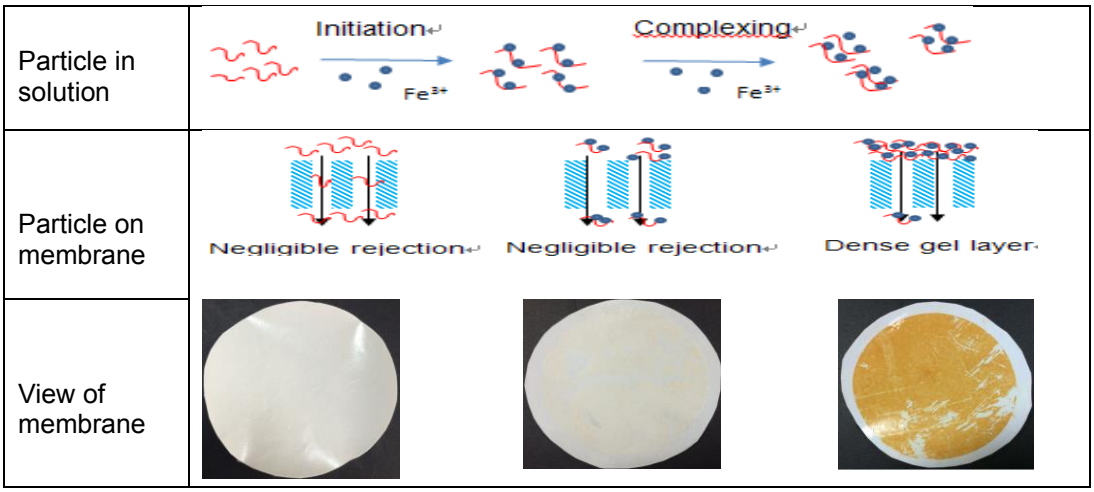

Fig. 12. Schematic illustration of interaction between ions and PAAS

After observing the membrane fouling type of different PAAS solutions, the specific resistance of cake was performed to further study the fouling degree and mechanism of PAAS solutions with different metal ion concentrations. From filtration theory based on Darcy's law, considering resistances in series, one obtains for the liquid flux,

$$J = \frac{1}{A}\frac{dV}{dt} = \frac{\Delta P}{\mu(R_m + R_c)} \quad (12)$$

where A is the membrane area, μ is the dynamic viscosity of water samples (Pa·s). Assumptions usually made are a) that the cake resistance is proportional to the solid mass deposited on the membrane surface, and b) that the cake filtration performance under constant pressure is characterized by an average specific resistance α (Aslam *et al.* 2015), so that,

$$R_c = \frac{\alpha c_b V}{A} \quad (13)$$

where $c_b$is the bulk concentration of particles (kg/m^3); Substituting Eq. 14 in Eq. 13 and integrating one obtains,

$$\frac{t}{V} = \frac{\mu\alpha C}{2\Delta P A^2} V + \frac{\mu R_m}{\Delta P A} \quad (14)$$

where t is the filtration time (s), and V is the filtrate volume (mL). By plotting the data as V against t/V, α can be obtained from the slope of the linear relationship. To ensure that the linear regression results in R^2 values larger than 0.9, only the straight portion of the plot was included in the regression (Sioutopoulos *et al.* 2010).

Listiarini *et al.* (2009) proposed the use of this quantity (α), termed modified fouling index (MFI), as a measure of the fouling propensity of filtered water. The quantity

$$I = \alpha c_b \quad (15)$$

called "fouling index" is considered a measure of the water fouling potential.

Figure 13 shows the values for the fouling index according to various ion concentrations. The values of I increased as the ion concentration increased. This conclusion corresponds to the results that the addition of metal ions causes severe fouling.

Figure 12 shows a sketch of membrane fouling at various ion concentrations. The complexation between PAAS and metal ions became obvious with the addition of metal ions, leading to larger organic aggregates rapidly adsorbing on the membrane surface (Khan *et al.* 2009; Jin *et al.* 2015). These results can be attributed to three reasons: firstly, the metal ions may bind with –COOH in the PAAS molecules and bridge PAAS molecules to form a cross-linked chelate cake layer, aggravating membrane fouling (Lin *et al*. 2001). Secondly, the addition of metal ions may neutralize the negative charge of organic matters, reducing the electrostatic repulsion between PAAS and the membrane surface. Mass PAAS matter became attached on the membrane surface during the early stage of filtration. Thirdly, increasing metal ion concentration and salting out may reduce the solubility of PAAS, increasing the hydrophobic effect of organic matter (Al-Degs *et al*. 2008). In this case, there is obvious attractive interaction between PAAS and the membrane surface, aggravating membrane fouling. Hence, cake layer formed at high ion concentrations and tended to be dense. This result suggests that the concentration of metal ions played a significant role in cake formation. The membrane fouling was aggravated with increasing metal ion concentration.

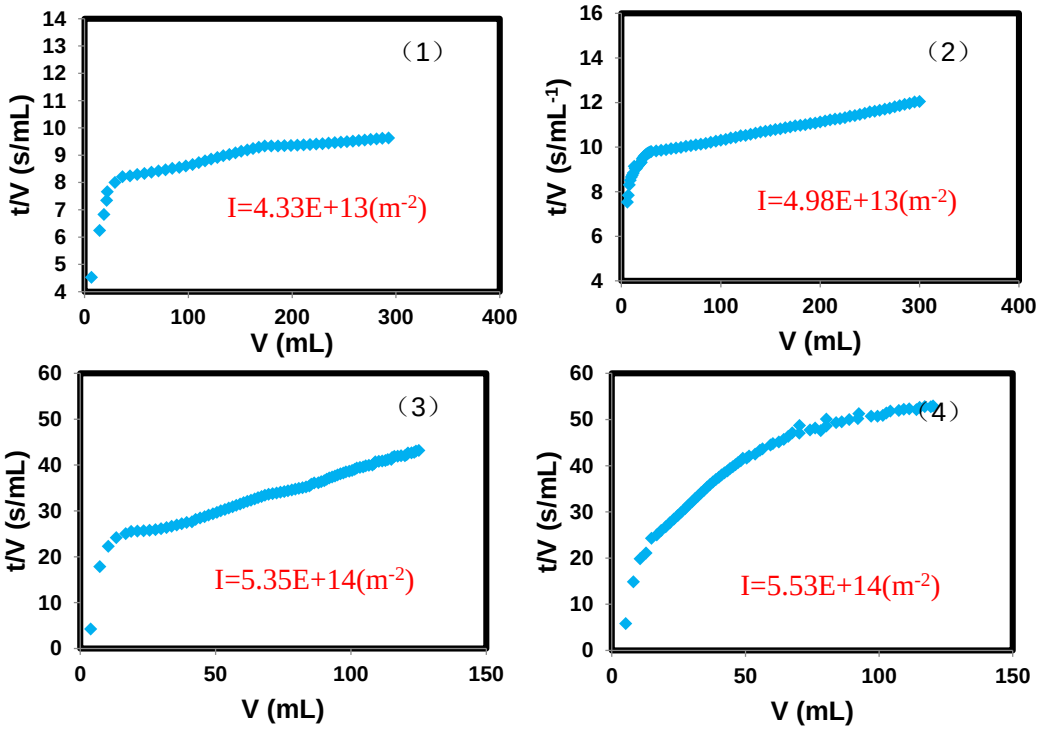

Fig. 13. Ratio of filtration time and filtration volume as a function of the total filtrate volume of the investigated systems: (1); PAAS+10 mM Ca(II); (2) PAAS+40 mM Ca(II); (3) PAAS+10 mM Fe(III); and (4) PAAS+30 mM Fe(III)

CONCLUSIONS

This paper put forward the mechanisms regarding the influence of dissolved organics in papermaking whitewater together with metal ions on the ultrafiltration (UF) membrane fouling and provided theoretical support to interactions between various metal ions and DOM in papermaking whitewater.

1. Increased pH values influenced the interaction between metal ions and dissolved organics, resulting in a slow membrane flux decline. The increase of Na^+ concentration reduced the particle size of organics and increased the membrane fouling to some extent.
2. Increasing concentrations of metal ions resulted in greater membrane fouling due to their chelation with dissolved organics.
3. For water samples with a high concentration of metal ions, gel layer formation played a major role in membrane fouling, whereas for solutions without metal ions, intermediate blocking formation was the major fouling mechanism.
4. The concentration of metal ions played a significant role in cake formation. Membrane fouling was aggravated with increasing metal ion concentrations for the higher values of the specific resistance of cake.

ACKNOWLEDGMENTS

The authors are grateful for the support of the National Natural Science Foundation of China (Grant No. 31270614) and the Priority Academic Program Development of Jiangsu Higher Education Institutions (PAPD).

REFERENCES CITED

Abdelrasoul, A., Doan, H., and Lohi, A. (2013). "A mechanistic model for ultrafiltration membrane fouling by latex," *Journal of Membrane Science* 433(15), 88-99. DOI: 10.1016/j.memsci.2013.01.003

Al-Degs, Y. S., Barghouthi, M. L., Sheikh, A. H., and Walker, G. M. (2008). "Effect of solution pH, ionic strength, and temperature on adsorption behavior of reactive dyes on activated carbon," *Dyes and Pigments* 77(1), 16-23. DOI: 10.1016/j.dyepig.2007.03.001

Ang, W. S., Lee, S. Y., and Elimelech, M. C. (2006). "Chemical and physical aspects of cleaning of organic-fouled reverse osmosis membranes," *Journal of Membrane Science* 272(1–2), 198-210. DOI: 10.1016/j.memsci.2005.07.035

Antony, A., Bassendeh, M., Richardson, D., Aquilina, S., Hodgkinson, A., Law, L., and Leslie, G. (2012). "Diagnosis of dissolved organic matter removal by GAC treatment in biologically treated paper mill effluents using advanced organic characterization techniques," *Chemosphere* 86(8), 829-836. DOI: 10.1016/j.chemosphere.2011.11.059

Ashrafi, O., Yerushalmi, L., and Haghighat, F. (2015). "Wastewater treatment in the pulp-and-paper industry: A review of treatment processes and the associated greenhouse gas emission," *Journal of Environmental Management* 158(1), 146-157. DOI: 10.1016/j.jenvman.2015.05.010

Aslam, M., Lee, P. H., and Kim, J. H. (2015). "Analysis of membrane fouling with porous membrane filters by microbial suspensions for autotrophic nitrogen," *Separation and Purification Technology* 146(26), 284-293. DOI: 10.1016/j.seppur.2015.03.042

Baguena, M. J. C., Blanco, S. A., and Vela, M. C. V. (2015). "Fouling mechanisms of ultrafiltration membranes fouled with whey model solutions," *Desalination* 360(16), 87-96. DOI: 10.1016/j.desal.2015.01.019

Chai, X. S., Samp, J. C., Yang, Q. F., Song, H. N., Zhang, D. C., and Zhu, J. Y. (2006). "Determination of microstickies in recycled whitewater by headspace gas chromatography," *Journal of Chromatography A* 1108(1), 14-19. DOI: 10.1016/j.chroma.2005.12.108

Chen, D., Weavers, L. K., and Walker, H. W. (2006). "Ultrasonic control of ceramic membrane fouling: Effect of particle characteristics," *Water Research* 40(4), 840-850. DOI: 10.1016/j.watres.2005.12.031

Chen, X. R., Luo, J. Q., Qi, B. K., Cao, W. F., and Wan, Y. H. (2015). "NOM fouling behavior during ultrafiltration: Effect of membrane hydrophilicity," *Journal of Water Process Engineering* 7, 1-10. DOI: 10.1016/j.jwpe.2015.04.009

Chon, K., Cho, J., and Shon, H. K. (2013). "Fouling characteristics of a membrane bioreactor and nanofiltration hybrid system for municipal wastewater reclamation," *Bioresource Technology* 130, 239-247. DOI: 10.1016/j.biortech.2012.12.007

Feng, B., Fang, Z., Hou, J. C., Ma, X., Huang, Y. L., and Huang, L. (2013). "Effects of heavy metal wastewater on the anoxic/aerobic-membrane bioreactor bioprocess and membrane fouling," *Bioresource Technology* 142, 32-38. DOI: 10.1016/j.biortech.2013.05.019

Garcia, A., Barrera, M., and Camacho, G. P. (2014). "Effect of pH, ionic strength, and background electrolytes on Cr(VI) and total chromium removal by acorn shell of *Quercus crassipes* Humb. and Bonpl.," *Environmental Monitoring and Assessment* 186(10), 6207-6221. DOI: 10.1007/s10661-014-3849-8

Guo, W. S., Ngo, H. H., and Li, J. X. (2012). "A mini-review on membrane fouling," *Bioresource Technology* 122, 27-34. DOI: 10.1016/j.biortech.2012.04.089

Habib, M., Habib, U., Memon, A. R., Amin, U., Karim, Z., Khan, A. U., Naveed, S., and Ali, S. (2013). "Predicting colloidal fouling of tap water by silt density index (SDI): Pore blocking in a membrane process," *Journal of Environmental Chemical Engineering* 1(1–2), 33-37. DOI: 10.1016/j.jece.2013.03.005

Hao, Y., Moriya, A., Ohmukai, Y., Matsuyama, H., and Matsuyama, T. (2013). "Effect of metal ions on the protein fouling of hollow-fiber ultrafiltration membranes," *Separation and Purification Technology* 111(25), 137-144. DOI: 10.1016/j.seppur.2013.03.037

Heidari, A., Younesi, H., Mehraban, Z., and Heikkinen, H. (2013). "Selective adsorption of Pb(II), Cd(II), and Ni(II) ions from aqueous solution using chitosan-MAA nanoparticles," *International Journal of Biological Macromolecules* 61, 251-263. DOI 10.1016/j.ijbiomac.2013.06.032.

Jiang, T., Zhang, H. M., Gao, D., Dong, F., Gao, J. F., and Yang, F. L. (2012). "Fouling characteristics of a novel rotating tubular membrane bioreactor," *Chemical Engineering and Processing: Process Intensification* 62, 39-46. DOI: 10.1016/j.cep.2012.09.012

Jin, Y. X., Ju, Y. G., Lee, H., and Hong, S. (2015). "Fouling potential evaluation by cake fouling index: Theoretical development, measurements, and its implications for fouling mechanisms," *Journal of Membrane Science* 490(15), 57-64. DOI: 10.1016/j.memsci.2015.04.049

Karabelas, A. J., and Sioutopoulos, D. C. (2015). "New insights into organic gel fouling of reverse osmosis desalination membranes," *Desalination* 368(15), 114-126. DOI: 10.1016/j.desal.2015.01.029

Khan, S. J., Visvanathan, C., and Jegatheesan, V. (2009). "Prediction of membrane fouling in MBR Systems using empirically estimated specific cake resistance," *Bioresource Technology* 100(23), 6133-6136. DOI: 10.1016/j.biortech.2009.06.037

Kloster, N., Brigante, M., Zanini, G., and Avena, M. (2013). "Aggregation kinetics of humic acids in the presence of calcium ions," *Colloids and Surfaces A: Physicochemical and Engineering Aspects* 427(20), 76-82. DOI: 10.1016/j.colsurfa.2013.03.030

Kumar, S., Guria, C., and Mandal, A. (2015). "Synthesis, characterization and performance studies of polysulfone/bentonite nanoparticles mixed-matrix ultra-filtration membranes using oil field produced water," *Separation and Purification Technology* 150(17), 145-158. DOI: 10.1016/j.seppur.2015.06.029

Lin, L. F., Liu, S. H., and Hao, O. J. (2001). "Effect of functional groups of humic substances on uf performance," *Water Research* 35(10), 2395-2402. DOI: 10.1016/S0043-1354(00)00525-X

Lin, T., Lu, Z. J., and Chen, W. (2015). "Interaction mechanisms of humic acid combined with calcium ions on membrane fouling at different conditions in an ultrafiltration system," *Desalination* 357(2), 26-35. DOI: 10.1016/j.desal.2014.11.007

Listiarini, K., Sun, D. D., and Leckie, J. O. (2009). "Organic fouling of nanofiltration membranes: Evaluating the effects of humic acid, calcium, alum coagulant and their combinations on the specific cake resistance," *Journal of Membrane Science* 332(1–2), 56-62. DOI: 10.1016/j.memsci.2009.01.037

Nguyen, T. A. H., Ngo, H. H., Guo, W. S., Zhang, J., Liang, S., Yue, Q. Y., Li, Q., and Nguyen, T. V. (2013). "Applicability of agricultural waste and by-products for adsorptive removal of heavy metals from wastewater," *Bioresource Technology* 148, 574-585. DOI: 10.1016/j.biortech.2013.08.124

Park, C., Kim, H., Hong, S. K., and Choi, S. (2006). "Variation and prediction of membrane fouling index under various feed water characteristics," *Journal of Membrane Science* 284(1–2), 248-254. DOI: 10.1016/j.memsci.2006.07.036

Pokhrel, D., and Viraraghavan, T. (2004). "Treatment of pulp and paper mill wastewater-A review," *Science of the Total Environment* 333(1–3), 37-58. DOI: 10.1016/j.scitotenv.2004.05.017

Rajabi, H., Ghaemi, N., Madaeni, S., Daraei, P., Astinchap, B., Zinadini, S., and Razavizadeh, S. H. (2015). "Nano-ZnO embedded mixed matrix polyethersulfone (PES) membrane: Influence of nanofiller shape on characterization and fouling resistance," *Applied Surface Science* 349(15), 66-77. DOI: 10.1016/j.apsusc.2015.04.214

Roger, G. M., Meriguel, G., Bernard, O., Durand, S., and Turq, P. (2013). "Effect of ionic condensation and interactions between humic substances on their mobility: An experimental and simulation study," *Colloids and Surfaces A: Physicochemical and Engineering Aspects* 436(5), 408-416. DOI: 10.1016/j.colsurfa.2013.07.007

Shamsuddin, N., Das, D. B., and Starov, V. M. (2015). "Filtration of natural organic matter using ultrafiltration membranes for drinking water purposes: Circular cross-flow compared with stirred dead end flow," *Chemical Engineering Journal* 276(15), 331-339. DOI: 10.1016/j.cej.2015.04.075

Sioutopoulos, D. C., Karabelas, A. J., and Yiantsios, S. G. (2010). "Organic fouling of RO membranes: Investigating the correlation of RO and UF fouling resistances for predictive purposes," *Desalination* 261(3), 272-283. DOI: 10.1016/j.desal.2010.06.071

Su, W. P., Chen, C., Zhu, Y. L., Yang, W. S., and Dai, H. Q. (2015). "Fouling characteristics of dissolved organic matter in papermaking process water on polyethersulfone ultrafiltration membranes," *BioResources* 10(3), 5906-5919. DOI: 10.15376/biores.10.3.5906-5919.

Tang, C. C., He, Z. W., Zhao, F. B., Liang, X. Y., and Li, Z. S. (2014). "Effects of cations on the formation of ultrafiltration membrane fouling layers when filtering fulvic acid," *Desalination* 352(3), 174-180. DOI: 10.1016/j.desal.2014.08.020

Tenno, R., and Paulapuro, H. (1999). "Removal of dissolved organic compounds from paper machine whitewater by membrane bioreactors: A comparative analysis," *Control Engineering Practice* 7(9), 1085-1099. DOI: 10.1016/S0967-0661(99)00079-9

Wang, L. L., Wang, L. F., Ye, X. D., Yu, H. Q. (2013). "Hydration interactions and stability of soluble microbial products in aqueous solutions," *Water Research* 47(15), 5921-5929. DOI: 10.1016/j.watres.2013.07.014

Wang, L., Wang, X. D., and Fukushi, K. (2008). "Effect of operational conditions on ultrafiltration membrane fouling," *Desalination* 229(1–3), 181-191. DOI: 10.1016/j.desal.2007.08.018

Wu, R. N., He, B. H., Zhao, G. L., and Li, X. F. (2014). "Immobilization of pectinase on polyethyleneimine-coated pulp fiber for treatment of whitewater from papermaking," *Journal of Molecular Catalysis B: Enzymatic* 99, 163-168. DOI: 10.1016/j.molcatb.2013.11.007

Yoon, Y. S., Lee, C. H., Kim, K. J., and Fane, A. G. (1998). "Effect of calcium ion on the fouling of nanofilter by humic acid in drinking water production," *Water Research* 32(7), 2180-2186. DOI: 10.1016/S0043-1354(97)00416-8

Zhang, X. L., Fan, L. H., and Roddick, F. A. (2013). "Understanding the fouling of a ceramic microfiltration membrane caused by algal organic matter released from *Microcystis aeruginosa*," *Journal of Membrane Science* 447(15), 362-368. DOI: 10.1016/j.memsci.2013.07.059

Zhang, R. J., Shi, W. X., Yu, S. L., Wang, W., Zhang, Z. Q., Zhang, B., and Bao, X. (2015). "Influence of salts, anion polyacrylamide and crude oil on nanofiltration membrane fouling during desalination process of polymer flooding produced water," *Desalination* 373(1), 27-37. DOI: 10.1016/j.desal.2015.07.006

Zhao, D. J., Lau, E., Huang, S., and Moraru, C. I. (2015). "The effect of apple cider characteristics and membrane pore size on membrane fouling," *LWT-Food Science and Technology* 64(2), 974-979. DOI: 10.1016/j.lwt.2015.07.001

Article submitted: August 30, 2015; Peer review completed: October 16, 2015; Revised version received: November 17, 2015; Accepted: November 20, 2015; Published: December 9, 2015.
DOI: 10.15376/biores.11.1.1108-1124